

# A Novel Transformation Watershed Image Segmentation Model in Digital Elevation Maps Processing

Aref Safari<sup>1\*</sup>

<sup>1</sup>Department of Computer Engineering, Islamic Azad University, Rasht Branch, Rasht, Iran

\*Email of Corresponding Author: Safari.aref@qodsiau.ac.ir

*Received: June 16, 2020; Accepted: August 23, 2020*

## Abstract

Computer analysis of image objects starts with finding them-deciding which pixels belong to each object. Digital elevation maps or models (DEMs) are arrays of numbers representing the spatial distribution of terrain elevations. They can be seen as gray-scale images, whereby the value of a pixel represents an elevation rather than a luminance intensity (the brighter the gray-tone level of a pixel, the higher the elevation of the terrain point corresponding to this pixel). Useful applications of DEMs can be found in civil/rural engineering, geographic information systems (GIS), geomorphology, water resources management, photogrammetry, satellite imaging. A watershed is defined as a region of land that assists in draining water (usually rainwater) into a river or a creek. It is an area of high ground through which water flows into the river or creek. Simply defined, the watershed is a transformation in grayscale images. This technique aims to segment the image, typically when two regions-of-interest are close to each other, their edges touch. Thus far, we have discussed segmentation based on three principal concepts.

## Key words

Image Processing, Maps Production, Watershed Algorithm, Computer-integrated Manufacturing Systems

## 1. Introduction

Image segmentation is one of the most important categories of image processing. The purpose of image segmentation is to divide an original image into homogeneous regions. It can be applied as a pre-processing stage for other image processing methods. There exist several approaches for image segmentation methods for image processing. The watershed transformation is studied in this report as a particular method of a region-based approach to the segmentation of an image. First, the basic tool, the watershed transform is defined. It has been shown that it can be implemented by applying the flooding process on a grey tone image. This flooding process can be performed by using basic morphological operations. The complete transformation incorporates a pre-processing and post-processing stage that deals with embedded problems such as edge ambiguity and the output of a large number of regions. Watershed Transform can be applied to grayscale images, textural images, and binary images. The watershed transform has been widely used in many fields of image processing, including medical image segmentation. A comprehensive review of hydrological, geomorphological, and biological applications of DEMs is proposed in [1]. A low-cost solution for generating a DEM consists of interpolating the elevation values between the elevation contour lines extracted from digitized topographic maps. For example, a sample of a digitized topographic map is shown in Figure 1a. The contour lines of this image can be automatically extracted using color

information. The resulting image is then cleaned using size criteria (surface area opening and closing). The filtered contour lines are then thinned using a skeletonization algorithm. Finally, disconnected lines are reconnected by considering the distance separating their extremities as well as their orientation. The resulting contour lines are shown in Figure 1b. Once the contour lines have been assigned their elevation value, it is still necessary to interpolate the elevation values of the points located in between two successive contour lines. The term watershed refers to a ridge that divides areas drained by different river systems. A catchment basin is a geographical area draining into a river or reservoir.

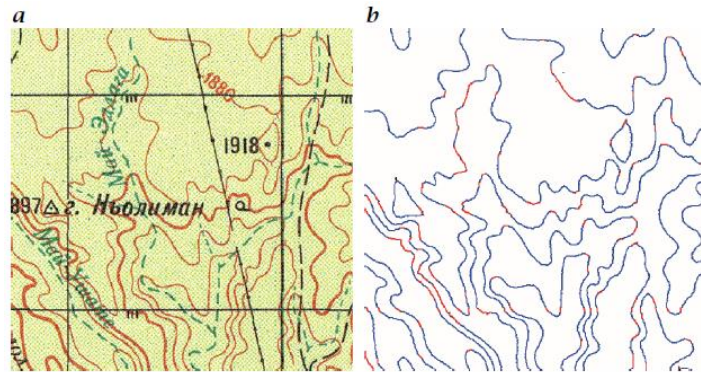


Figure 1. a) Digitized topographic map; b) extracted contour lines

A larger image of elevation contour lines is shown in Figure 2: each line has a constant gray-scale value corresponding to the terrain elevation along the line and the elevation values of the pixels belonging to white regions in between two successive contour lines are unknown. In this problem, contour lines are associated with terrain elevation values but they could represent other spatial-dependent characteristics of an object. For instance, one could transform a gray-tone image into an image of iso-intensity contour lines and then attempt to regenerate the original image (i.e., lossy image compression technique). There is, therefore, a need for interpolating values located in between successive contour lines. Geodesic transformations are at the basis of an efficient method taking advantage of the topological and morphological properties of the contour lines. The method requires two steps:

i) Generation of two plateau images, and ii) interpolation along the steepest slope lines.

## 2. Research Background

Segmentation divides an image into its constituent regions or objects, and the segmentation must be stopped when the objects of interest in an application have been isolated [1]. Image segmentation is based on three principal concepts: edge detection, thresholding, and region growing. The most common one is thresholding. Thresholding has a high speed of operation and ease of implementation. However, its performance is relatively limited since image pixels with the same gray level value will invariably be segmented into the same class [2]. Segmentation by morphological watersheds [3–10] embodies many of the concepts of the other three approaches, which produces more stable segmentation results, as well as providing a simple framework. A simple watershed transformation causes over-segmentation [11]. In order to prevent this over-

segmentation, the watershed method passed through several stages of evolution. The original watershed method was developed in [12] and was widely described together with its applications by some other researchers [13, 14]. The result of the enhancement by imposing regional minima at the locations of both the internal and the external markers, combine the top/bottom hat transformation algorithm and the markers algorithm by using suitable weight function, and subject the combination to the watershed algorithm. The new algorithm can prevent over-segmentation of the simple watershed segmentation algorithm. The other particularity of the proposed algorithm is insensitivity to noise.

One of the principal applications of watershed segmentation is in the extraction of nearly uniform (blob-like) objects from the background. Regions characterized by small variations in intensity have small gradient values. Thus, in practice, we often see watershed segmentation applied to the gradient of an image, rather than to the image itself. In this formulation, the regional minima of catchment basins correlate nicely with the small value of the gradient corresponding to the objects of interest. The earlier methods of transformation treat the image as a topographic map, with the intensity of each pixel representing the height. For instance, dark areas can be intuitively considered to be ‘lower’ in height and can represent troughs. On the other hand, bright areas can be considered to be ‘higher’, acting as hills or as a mountain ridge. Any gray tone image can be considered as a topographic surface. If we flood this surface from its minima and, if we prevent the merging of the waters coming from different sources, we partition the image into two different sets: The catchment basins and the watershed lines. If we apply the watershed transformation to the image gradient, the catchment basins should theoretically correspond to the homogeneous gray level regions of this image. However, in practice, this transform produces an important over-segmentation due to noise or local irregularities in the gradient image. To perform image segmentation and edge detection tasks, many methods incorporate region growing and edge detection techniques. For example, it is applying edge detection techniques to obtain Difference in Strength (DIS) map. Then employ region growing techniques to work on the map as in [2]. According to the paper [3], combining both special and intensity information in the image segmentation approach based on multi-resolution edge detection, region selection, and intensity threshold methods to detect white matter structure in the brain. In [3, 6, 7, 9] adaptive clustering algorithm and K-means clustering algorithm are generalizing to include spatial constraints and to account for local intensity variations in the image. The spatial constraints are included by the use of a Gibbs Random Field model (GRF). In such a “topographic” interpretation, we consider three types of points: (1) points belonging to a regional minimum; (2) points at which a drop of water, if placed at the location of any of those points, would fall with certainty to a single minimum; and (3) points at which water would be equally likely to fall to more than one such minimum. For a particular regional minimum, the set of points satisfying condition (2) is called the catchment basin or watershed of that minimum. The points satisfying condition (3) form crest lines on the topographic surface, and are referred to as divider lines or watershed lines.

### **3. Mathematical Model of Proposed Method**

The watershed segmentation algorithms are based on the representation of an image in the form of a topographic relief, where the value of each image element characterizes its height at this point.

These algorithms can process not only 2D images but also 3D images, so the term element is used in the paper to combine the terms pixel and voxel. For a better outcome, watershed segmentation is often applied to the result of the distance transform of the image rather than to the original one. Thus, the relief consists of low-lying valleys (minimums), high-altitude ridges (watershed lines) and slopes (catchment basins). The concept of the plateau (an area with the same height of elements) is also used. The main task in this segmentation method is to determine the location of all catchment basins and/or watershed lines since in this case, each catchment basin is considered to be a separate segment of the image. In some tasks, we only need to get the segments, but in some, we also need to know the boundaries of each segment.

So, let  $M_1, M_2, \dots, M_R$  be set denoting the coordinates of the points in the regional minima of an image,  $g(x, y)$ . As mentioned earlier, this typically will be a gradient image. Let  $C(M_i)$  be a set denoting the coordinates of the points in the catchment basin associated with regional minimum  $M_i$  (recall that the points in any catchment basin form a connected component). The notation  $\min$  and  $\max$  will be used to denote the minimum and maximum values of  $g(x, y)$ . Finally, let  $T[n]$  represent the set of coordinates  $(s, t)$  for which  $g(s, t) < n$ . That is,

$$T[n] = \{(s, t) | g(s, t) < n\} \quad (1)$$

Geometrically,  $T[n]$  is the set of coordinates of points in  $g(x, y)$  lying below the plane  $g(x, y) = n$

In this work, A magnified section of an image of contour lines is shown in Figure 3a. The pixel  $p$  lies within a white region surrounded by two contour lines referred to as its lower and upper contour lines. The lower contour line of a pixel  $p$  is denoted by  $C_l(p)$  and the upper one by  $C_u(p)$ . These two contour lines may be identified as shown in Figure 3b or when  $p$  is located precisely on a contour line. The elevation of both the lower and upper contour lines associated with each pixel is determined by calculating two plateau images  $P_l$  and  $P_u$  from the image  $CL$  of Contour Lines:

$$P_l(p) = CL[C_l(p)] \quad (2)$$

$$P_u(p) = CL[C_u(p)] \quad (3)$$

Hereafter, we assume that the image  $CL$  of contour lines has values strictly greater than 0 along the contour lines, the remaining pixels being set to 0. The computation of the plateau images requires the definition of the following image  $M$ :

$$M(P) = \{C_l(p) \text{ if } p \text{ belongs to a counter line}\} \quad (4)$$

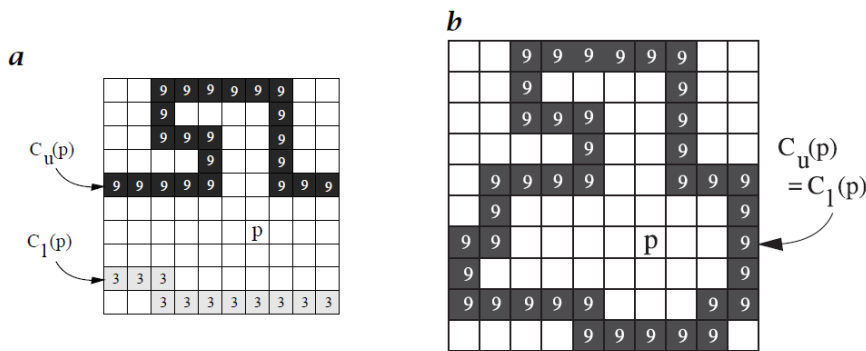


Figure 2. Magnified section of an image of iso-intensity contour lines with a pixel  $p$  located in a white region

The plateau images are then obtained by performing a morphological reconstruction by the erosion of  $CL$  from  $M$  for the lower plateau image  $P_l$  and a morphological reconstruction by dilation of  $M$  from  $CL$  for the upper plateau image  $P_u$ :

$$P_l = R_{CL}(M) \quad (5)$$

$$P_u = R_M(C_l) \quad (6)$$

The proposed morphological reconstruction algorithms have been used for generating a pair of plateau images starting from an image of elevation contour lines. This was the first step towards the interpolation of the elevation values of the pixels located between two successive contour lines. The second step consists in calculating the value of each pixel  $p$  by a linear interpolation along the geodesic going from its upper contour line  $C_u(p)$  to its lower contour line  $C_l(p)$  and passing through  $p$ .

A magnified section of an image of contour lines is shown in Figure 4. In the figure, a pixel  $p$  located in between its upper and lower contour lines is drawn with the corresponding geodesic linking the pixel to both contour lines. The shortest path going from  $C_u(p)$  to  $C_l(p)$ , included in  $M$  and passing through  $p$ , is made of the geodesics from  $p$  to  $C_l(p)$  and from  $p$  to  $C_u(p)$ . We assume that the difference of elevation between  $C_u(p)$  and  $C_l(p)$  is evenly distributed along the geodesic path. The interpolated value  $H(p)$  of  $p$  equals, therefore, the weighted mean of  $P_u(p)$  and  $P_l(p)$  by the geodesic distances from  $p$  to  $C_u(p)$  and to  $C_l(p)$ , respectively:

$$H(p) = \frac{P_l(p) d_M[p, C_u(p)] + P_u(p) d_M[p, C_l(p)]}{d_M[p, C_l(p)] + d_M[p, C_u(p)]} \quad (7)$$

where the geodesic mask  $M$  is the set difference between the image definition domain and the contour lines, and  $P_u$  and  $P_l$  are the plateau images defined in the earlier section. The length of the geodesics linking each pixel to its upper and lower contour lines is determined from two geodesic distance functions: from odd to even contour lines and vice versa (odd contour lines are obtained by considering one contour line out of two and starting from the contour line at the lowest level).

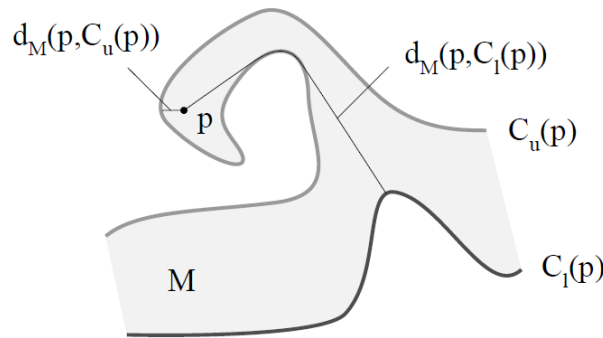


Figure 3. Interpolation of the value

### 3.1 Marker Control and Measuring Image Information

Direct application of watershed transform to a gradient image can result in over-segmentation due to noise. Over segmentation means a large number of segmented regions. An approach used to control over-segmentation is based on the concept of markers. A marker is a connected component belonging to an image. Markers are used to modify the gradient image. Markers are of two types internal and external, internal for an object, and external for boundary [7]. The marker-controlled

watershed segmentation is a robust and flexible method for the segmentation of objects with closed contours, where the boundaries are expressed as ridges. Markers are placed inside an object of interest; internal markers associate with objects of interest and external markers associated with the background. After segmentation, the boundaries of the watershed regions are arranged on the desired ridges, thus separating each object from its neighbors [1,8]. Its fundamental premise is that the generation of information can be modeled as a probabilistic process that can be measured in a manner that agrees with intuition. Following this supposition, a random event  $E$  with probability  $P(E)$  is said to contain:

$$I(E) = \log \frac{1}{P(E)} = -\log P(E) \quad (8)$$

units of information. If  $P(E) = 1$  (that is the event always occurs),  $I(E) = 0$  and no information is attributed to it. Because no uncertainty is associated with the event, no information would be transferred by communicating that the event has occurred where it always happens if  $P(E) = 1$ .

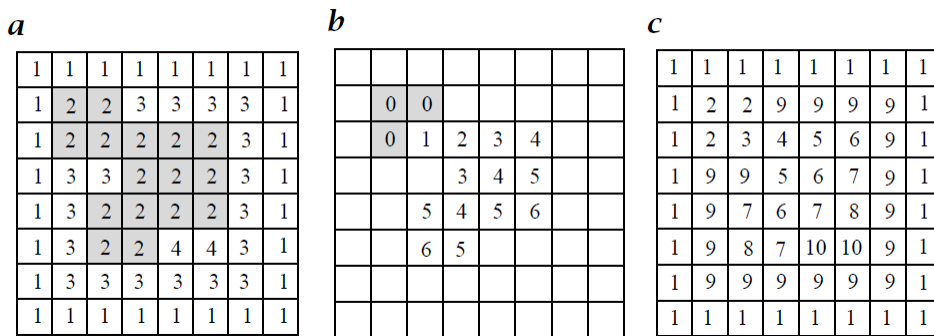


Figure 4. Lower complete transformation: a) original gray image; b) geodesic function and c) lower complete image.

#### 4. Experimental Results and Performance Evaluation

In this section, we present the experimental results to demonstrate the performance of the watershed technique. The performance of the method under the presence of intense noise is also analyzed, and the results are compared with other segmentation methods. When a pixel drains towards another, the *result* of the latter is incremented by that of the former. The process is then repeated for the second-highest elevation and so forth until the lowest elevation is reached. When a pixel has more than one neighbor at the lowest elevation, one of them is chosen randomly to avoid systematic errors. The resulting image of contributing drainage areas is shown in Figure 6. This image can be thresholds at a user-defined value  $S$  to extract the drainage network pixels draining at least  $S$  pixels. Figure 5 shows the drainage networks for various threshold levels. Figure 6 illustrates the lower complete transformation with a perspective view of plateaus and its lower complete version. Note that values of points higher than the plateau are increased by the largest computed geodesic distance. Consequently, the resulting DEM has more levels than the original one but ordered relationships between pixels are preserved. The lower complete transformation can be achieved utilizing sequential algorithms. The result of the watershed algorithm is global segmentation, border closure, and high accuracy. It can achieve a one-pixel wide, connected, closed, and exact location of the outline. The basic concept of the watershed is based on visualizing a gray level image into its topographic representation, which includes three basic notions: minima, catchment basins, and watershed lines.

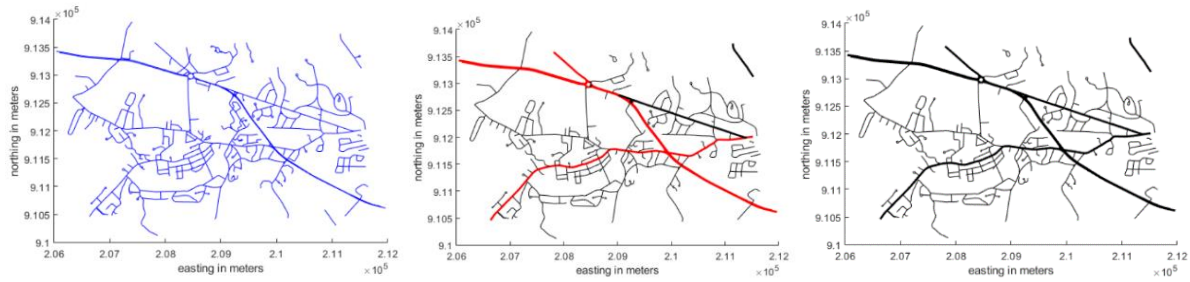


Figure 5. Concord Roads with proposed transformation model

Except for graph cuts and proposed watershed transformation in the segmentation process, the material in the previous section dealt mostly with what we might call “non-traditional” segmentation method, based primarily on detecting intensity discontinuities or similarities. In this work, we discuss techniques that approach segmentation from a “modeling” point of view. Specifically, we develop methods whose origin can be traced to work on deformable models conducted in the 1990s. Deformable watershed models are physically based models of deformable curves, surfaces, and solids used non-traditionally in computer graphics. In this research, a novel transformed watershed active contour (also called evolving fronts or evolving interfaces), has been proposed which is a deformable model and confined to the plane. The term “active” indicates that the curves are dynamic, as opposed, for example, to segmentation curves resulting from a global thresholding operation. In segmentation, these active curves are attracted to region boundaries, acting under the influence of forces extracted typically from an image being segmented. Work on active contours related specifically to image segmentation evolved along two different paths. Statistical evaluation of analytic performance in general and specifically ROC curve analysis was conducted for calculating the performance of proposed transformed watershed. The confusion matrix was calculated to define the performance of the suggested approaches. The confusion matrix describes all possible results of forecasting results in the table structure.

**Specificity:** The prospect of the test finding the correct class among all classes:

$$\frac{TN}{TN+FP} \quad (9)$$

**Accuracy:** The fraction of test results in those are correct:

$$\frac{TP+TN}{TP+FN+TN+FP} \quad (10)$$

Table-1 Geographic Cells Reference with properties

Parameter	Ranges	Performance
Latitude Limits	[44.2475 44.37775]	89%
Longitude Limits	[-71.38025 - 71.24525]	86%
Raster Size	[521 540]	-
Raster Interpretation	Cells	92%
Columns Start From	South	93%
Rows Start From	West	91%
Cell Extent in Latitude	1/4000	90%
Cell Extent in Longitude	1/4000	90%
Raster Extent in Latitude	0.13025	84%
Raster Extent in Longitude	0.135	88%
X Intrinsic Limits	[0.5 540.5]	91%
Y Intrinsic Limits	[0.5 521.5]	91%
Coordinate System Type	Geographic	-
Angle Unit	Degree	-
Specificity	-	92%
Accuracy	-	94%



Figure 6. Remotely sensed image of a part of Strasbourg (France)

## 5. Conclusion

Watershed transform is a powerful tool for image segmentation. However, the purpose of the watershed transform is not limited in image segmentation. In this paper, we have overviewed and



measured the expended computational resources of the watershed segmentation algorithms that are implemented in some open source libraries. We identified two libraries that showed the best results in our tests. Thus, for the best performance of the watershed segmentation, one should try different implementations from modern versions of libraries and choose the one that consumes the least computing resources, even though most of them contain implementations of the same algorithms. With this testing, one can already achieve a significant increase in performance for some problems, when the memory becomes a crucial issue, the only appropriate solution is splitting of the initial image into smaller parts, segmenting of these parts in parallel and following the merging of results. Even in this case, the performance of the segmentation algorithm implementation plays a significant role, since each part of the image must be processed with minimal computational resources. To solve the over-segmentation and noise sensitiveness of the simple watershed transform, the new algorithm is proposed in this paper. The proposed segmentation algorithm was implemented for several images and produced very satisfactory results with respect to suppression of over-segmentation. The appropriate weight function is used to combine the enhanced final multi-scale gradient algorithm with markers algorithm to get the new algorithm. A combination of these two algorithms can contribute to overcome the over-segmentation and under segmentation which is caused by enhanced final multiscale gradient algorithm and markers algorithm, respectively. The experimental results show that the new algorithm is superior to the final multiscale watershed segmentation model with an average accuracy of 94%.

## 6. References

- [1] Suetens, P., Fua, P. and Hanson, A.J. 1992. Computational Strategies for Object Recognition. *ACM Comput. Surv.* 24:5–62.
- [2] Bomans, M., Hohne, K.H., Tiede, U. and Riemer, M. 2009. 3-D segmentation of MR images of the head for 3-D display. *IEEE Trans. Med. Imaging.* 9:177–183.
- [3] McAuliffe, M.J., Lalonde, F.M., McGarry, D., Gandler, W., Csaky, K. and Trus, B.L. 2012. Medical Image Processing, Analysis and Visualization in clinical research. In Proceedings of the 14<sup>th</sup> IEEE Symposium on Computer-Based Medical Systems, CBMS 2012. 381–386.
- [4] Hsu, W.Y. 2015. Segmentation-based compression: New frontiers of telemedicine in telecommunication. *Telemat. Inf.* 32, 475–485.
- [5] Natale, F.G.B.D., Desoli, G.S., Giusto, D.D. and Vernazza, G. 2005. Polynomial approximation and vector quantization: a region-based integration. *IEEE Trans. Commun.* 43:198–206.
- [6] Pham, D.L., Xu, C. and Prince, J.L. 2000. Current Methods in Medical Image Segmentation. *Annu. Rev. Biomed. Eng.* 2:315–337.
- [7] Atta-Fosu, T., Guo, W., Jeter, D., Mizutani, C.M., Stopczynski, N. and Sousa-Neves, R. 2016. 3D Clumped Cell Segmentation Using Curvature Based Seeded Watershed. *Journal of Imaging.* 2(4):31-37.
- [8] Safari, A., Hosseini, R. and Mazinani, M. 2017. A Novel Type-2 Anfis Classifier for Modelling Uncertainty in Prediction of Air Pollution Disaster, *IJE Transactions B: Applications.* 30(11):1568-1577.

- [9] Safari, A., Barazandeh, D. and Khalegh Pour, S.A. 2020. A Novel Fuzzy-C Means Image Segmentation Model for MRI Brain Tumor Diagnosis. *Journal of Advances in Computer Engineering and Technology*. 6(1): 19-2
- [10] Meyer, F. Minimum Spanning Forests for Morphological Segmentation. 2017. *Mathematical Morphology and Its Applications to Image Processing*. Springer: Dordrecht, Netherlands. 77-84.
- [11] Wang, D. , 1997. A multiscale gradient algorithm for image segmentation using watersheds. *Pattern Recognition*. 30(12):2043–2052.
- [12] Gonzalez, R. C. and Woods, R. E. 2020. *Digital Image Processing*, Publishing House of Electronics Industry, Beijing, China, 3rd edition.
- [13] Jalba, A. C., Wilkinson, M. H. F. and Roerdink, J. B. T. M. 2019. Morphological hat-transform scale spaces and their use in pattern classification. *Pattern Recognition*. 37(5):901–915.
- [14] Jalba, A. C., Roerdink, J. B. T. M. and Wilkinson, M. H. F. 2013. Morphological hat-transform scale spaces and their use in texture classification. *Proceedings of the IEEE International Conference on Image Processing*. Orlando, USA.